Journal of Aeronautics, Astronautics and Aviation, Vol. 55, No. 3S, pp. 415 – 423 (2023)
DOI: https://doi.org/10.6125/JoAAA.202309_55(3S).01

The Aerodynamic Lift Performance Analysis of Channel-Wing Design for STOL Aircraft

Jasvinraj Sivapalan [1], Azmin Shakrine Mohd Rafie [1], Abd Rahim Abu Talib [1], Ezanee Gires [1, 3], Adi Azriff Basri [1, 3], Fairuz Izzuddin Romli [1, 2], Ahmad Salahuddin Mohd Harithuddin [1, 3], Sharizal Ahmad Sobri [4], Mohd Faisal Abdul Hamid [1, 2, 3 *]

[1]*Department of Aerospace Engineering Universiti Putra Malaysia, Serdang, Selangor, Malaysia*
[2]*Aerospace Design and Applications Research Work Group*
[3]*Aerospace Malaysia Research Centre (AMRC), UPM, Serdang, Malaysia*
[4]*Faculty of Bioengineering & Technology, Universiti Malaysia Kelantan, Jeli, Kelantan, Malaysia*

ABSTRACT

The use of Short Take-Off and Landing (STOL) aircraft with an upwardly opening semi-cylindrical channel, known as a channel-wing, is one of the best candidates for short-haul flights. The channel-wing utilized the entrainment of airflow on the inside of the wing channel, enhancing the pressure difference on the wing surfaces, boosting the generation of lift. The present study is aiming to acquire the aerodynamic performance for a new design; the propulsion unit is position behind the wing. The analysis is done experimentally with a 3D-printed model. The aircraft wing model is constructed with NACA 4412 profile, a wingspan of 400 mm, and a U-shape-channel diameter of 68 mm. Tested in an open loop wind tunnel at speed of up to 22 m/s, and angle of attack of up to +20 degrees. The result shows the lift coefficient can reach beyond 3, higher than those obtained by the conventional wing design. Also, it can delay the wing stall; the lift can be maintained beyond which the usual state (angle of attack) where the typical wing begins to stall. Indeed, the new channel-wing design is a good option to be considered, offers higher lift, and rises with speed. It generates more lift than conventional aircraft equipped with modern high-lift systems and outperforms the existing traditional channel-wing design, which is advantageous for short-haul flight.

Keywords: Short-haul flights, Channel-wing, Aerodynamic performance

I. INTRODUCTION

Air transport is the fastest mode of transportation; facilitate movement of resources and wealth between regions, countries, and city centers. The demand for air transport has shown a significant growth in recent years [1-2]. Inevitably, the statistic [3] has shown that both in the US and EU, the percentages of flight delay is ranging between 15 to 20 percent each year, and most of it is the short-haul flight. In addition, as highlighted by some studies [4-6], in the US for an example, the airline flight delay has incurred a staggering direct operating cost of about 8 billion USD per year. There are several factors that could lead to this problem, and one of them is most hub airports are heavily congested. This signifies a serious problem, especially to those who took the connecting flight, consequently, the airlines will suffer additional delay compensation costs.

At present, there are wide range of research have been carried out to mitigate these problems. Some are looking into possibilities to optimize the taxiway capacity and runway separation by developing a model that could help in simulating the problem of airline flight delay management which constraints by several factors, including the runway capacity [7-8]. And others are looking into minimizing the impact of aircraft wake vortex

Manuscript received, February 13, 2023, final revision, April 20, 2023
* To whom correspondence should be addressed, E-mail: mohd_faisal@upm.edu.my

generated by the other aircraft during arrival and departure. This eventually helps in optimizing the usage of runway capacity at any given time [9-13]. While there are also studies to consider some new elements in the design for future aircraft [14-20], includes the propulsion system and the geometrical shape of the aircraft, to make it more aerodynamic and cost effective in the long run.

Altering the conventional wing is the key for future aircraft design, it brings a greater option to alleviate some of the present problems, including the issues of short-haul flight. As the existing wing design limits the potential and capability in generating lift. The integrations of active flow control technology to enhance the aerodynamic performance of the wing is one of the best option to be considered [21-24].

This design, so called channel-wing aircraft (Figure 1), utilized the airflow entrainment to increase the generation of lift. Unlike conventional fixed wing aircraft that rely on the speed of the aircraft to generate lift, in contrast, the channel-wing utilized the airflow velocity passing over the wing; the airflow entrains on the inner part of the wing channel, induced by the high-speed rotating propeller. In return, boosting the generation of lift, by increasing the pressure difference between the inner (upper) and outer (lower) part of the wing, even when the aircraft is at stand still [25].

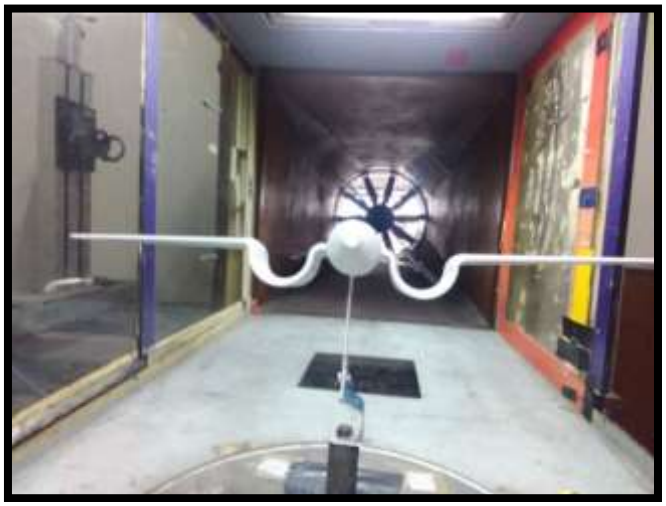

Figure 1 Front view of the 3D-printed channel-wing aircraft model in the wind tunnel

Previously, an experimental study has been carried out to assess the effect of wing sizing (chord length) on the aerodynamic lift and propulsive thrust performances of channel-wing aircraft at stand still conditions [26]. The analysis was done on three wings, namely small, medium, and large, which categories by the differences in the wing chord length. From the analysis, the larger wing is superior at energizing the lifting force, and the wing able to extract about 30% of the lift from the thrust.

Additionally, from the study perform at Georgia Tech Research Institute [23], it has shown the channel-wing could produce lift that is almost double than the conventional aircraft which is equipped with slotted flap. And, based on this, they have predicted that the channel-wing aircraft could perform take-off at under 100 ft of ground rolls, relatively very low compared to the conventional aircraft.

Given the remarkable performance of the channel-wing, Chang et al. [27] proposed and explored a different setup of the design, employing tandem channel-wing configurations for the electric vertical take-off landing aircraft (eVTOL). The results demonstrate that the aerodynamic performance is good; nevertheless, the downwash effect from the front wing influences the rear wing. This emphasizes the importance of uninterrupted airflow to ensure the aircraft's stability.

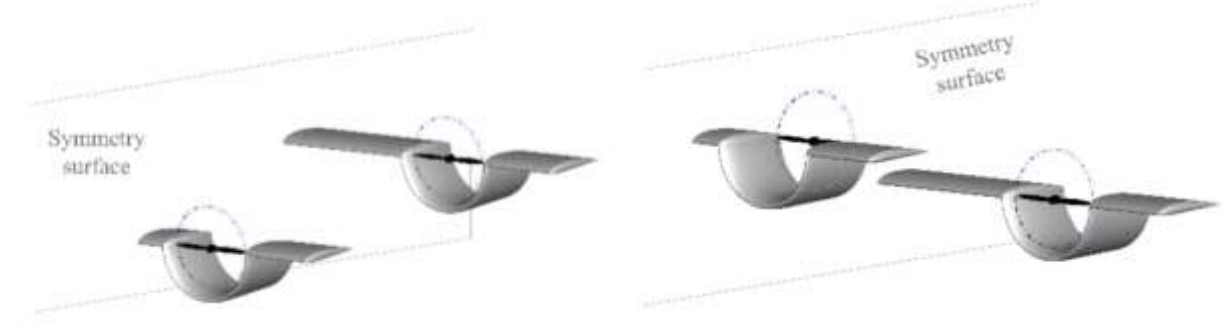

(a) front wing lower than rear wing (b) front wing upper than rear wing

Figure 2 Sketch of the tandem channel-wing configuration. Adapted from Ref. [27]

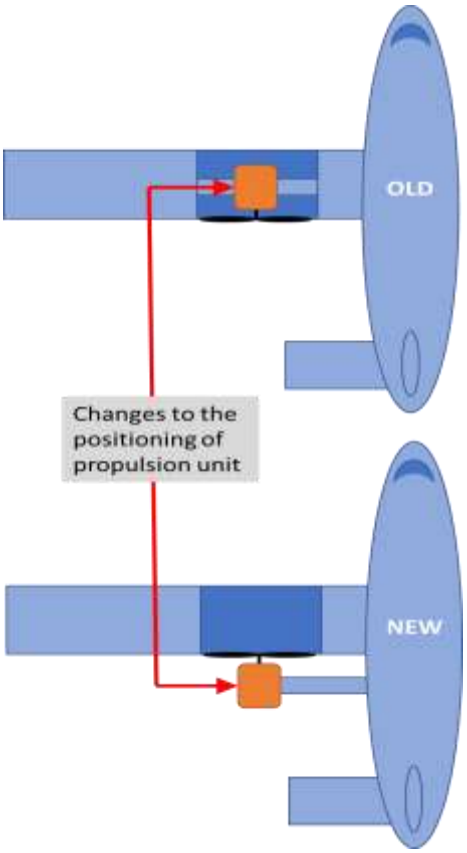

Figure 2 Position of propulsion unit (old vs new)

Gunther et al. [28] investigated the aerodynamic performance characteristics of channel-wing, comparing experimental results to the theoretical model published by Blick & Homer [25]. Their findings demonstrated that the theoretical model, for a range of test, could not predict channel-wing performance characteristics well. Moreover, data indicate that the performance of a channel-wing drops with increasing flight speed. This might, however, be owing to the influence of the propulsion unit, which was located on the inside and relatively closer to the channel-wing surface. The region (gap) between the propulsion unit and the channel-wing is narrow, and the blockage effect grows as speed increases, analogous to biplane aircraft conditions [29-31]. Aerodynamic interference occurs when the high-pressure air beneath the propulsion unit and the low-pressure air above the channel-wing interact. It has a major effect on both attached flow and lift production, which both decrease as the wings move closer together. This would have a significant impact on the formation of a low-pressure region on the inside of the channel-wing.

Indeed, from the aerodynamic performance point of view, channel-wing design is a good option to be considered and implemented for future STOL aircraft [32,33]. Nevertheless, the undisturbed airflow on the inside of the wing channel is critical and further analysis is required. In particular for the current design, i.e. with relocation of the propulsion unit to the rear part of the wing. The existing channel-wing design used the inner section to mount/locate the propulsion unit, while the current design model relocates and places it on the outside part behind the propeller (as illustrates in Figure 2 and shown in Figure 5 for the actual test model). This could improve entrainment and maintain the airflow from the leading-edge to the trailing-edge of the wing undisturbed, enhancing the formation of a low-pressure region for greater lift output.

Expanding form earlier work [26], this paper will be focusing on the analysis of the new design (propulsion unit behind the wing) of channel-wing aircraft performance for a range of flight speed at different angle of attack. The goal is to expand understanding of the channel-wing lift performance characteristics on the new design for future short-haul flight applications.

The test model is design using CAD software, consist of several main components to form the aircraft model. All the parts are made of PLA material, fabricated using the 3D printer, and assembled with metal (rod) insert. The study is performed for free-stream speeds up to 22 m/s and angles of attack up to +20 degrees; beyond this range, the wing vibrates (flutter). This problem limits the analysis, may cause damage to the wing structure, and may pose a risk to the wind tunnel itself. The experimental test setup is like the one presented earlier, i.e., here, a scaled-down model of the actual aircraft is used, with the propulsion unit is repositioned behind the wing.

II. SETUP AND METHODOLOGY

The analysis is done for Reynold number range of between 12k and 100k. Flow chart for the experimental analysis of the channel-wing aircraft model is shown in Figure 3 below,

In this experiment, the fuselage is design with a ratio of $\frac{2}{45}$ from the original aircraft size [25]. The original size of the fuselage is 9000 mm, which later reduced to a length of approximately to 400 mm. Scaling of the model is done to get a good proportion to the cross-sectional area of the wind tunnel test section. This helps in minimizing the blockage effect, and it was position higher (40 cm) from the floor of the wind tunnel test section, mainly to prevent ground effect. The general dimension of the test model is given in Table 1.

Model Design

Table 1 General dimension of the model

Part	Dimension
Fuselage	▪ Length: 395mm ▪ Max. Diameter: 59mm
U-shape-wing Section	▪ Diameter: 68mm ▪ Chord Length: 77mm
Wing	▪ Wingspan: 400mm ▪ Aspect Ratio: 11 ▪ Root-Chord: 77mm ▪ Tip-Chord: 38 mm

The CAD model of the channel-wing aircraft is shown in Figure 4; top left is the front view, bottom left is the isometric view of the channel-wing section, top right is the side view, and bottom right is the 3D view of the channel-wing aircraft model. The main body parts of the channel-wing aircraft model were divided into several smaller sections, and the whole aircraft geometry is based on the sizing given in Ref. [25].

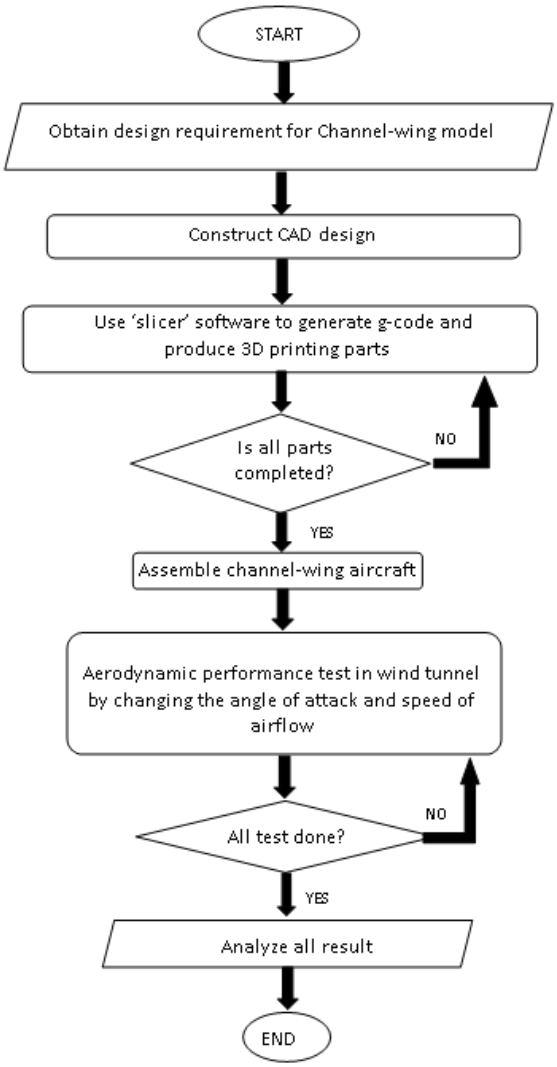

Figure 3 Flow chart for the experimental analysis of the channel-wing aircraft model

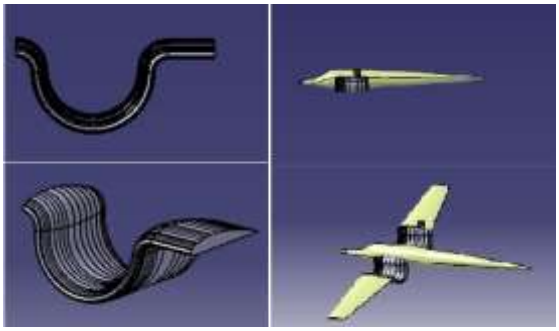

Figure 4 The CAD model of the channel-wing aircraft

Model Fabrication

Next, once all 3D CAD data has been exported to the 3D printer slicer software, the model fabrication process can begin. The slicer software is used to generate the G-Code. A thin layer of filler is used to cover all imperfections and close unneeded surface gaps. A small metal rod is inserted to each part and epoxy glue is applied to join all part sections, ensuring permanent bonding and rigidity. The test model fitting before assembly process is shown in Figure 5.

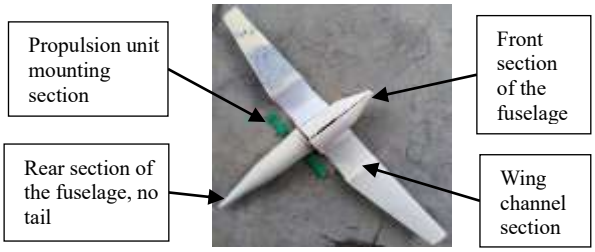

Figure 5 The test model fitting before assembly process

A customized extension of mounting stand is built to keep the channel-wing aircraft model stable inside the wind tunnel test section. This extended mounting stand is made of three layers of metal that were joined together with metal epoxy and attached to the lower part of the fuselage. They were later installed on the mounting base in the wind tunnel's test section for the following process: integration with electronic systems and cables to control the motor propeller.

Wind Tunnel Setup

Figure 6 A scale model of the actual open-loop wind tunnel

The open loop wind tunnel used for this test section is shown in Figures 6 (specification of the open-loop wind tunnel is given in Table 2), with ambient air sucked from the front opening of the wind tunnel inlet section (through the 5 layers of mesh) by a set of 10 bladed propellers at the rear end (outlet) of the wind tunnel. First, a series of calibration tests are performed prior to wind tunnel testing. This is done to ensure the accuracy and repeatability of the measured results, as well as to determine the correlation between the speed of the wind tunnel propeller blades and

the speed of the airflow inside the wind tunnel test section. The six-component force balance system is used to measure lift force. It is done over a predetermined angle of attack range of -10 to +20 degrees, by pitching the aircraft model. Data were collected at 5-degree intervals.

Table 2 Specification of the open-loop wind tunnel

Test section	1000 x 1000 x 2500 mm
Max. speed	50 m/s
Power available	75 Hp
Anti-turbulent screen	4 sheets
Number of blades	10 blades
Overall length	14.5 meters
Overall height	4 meters

The airflow speed inside the test section of the wind tunnel is measured at two locations using two digital manometers: positions at the front and in the middle of the test section. The calibrated airflow speed is measured by varying/adjusting the wind tunnel propeller speed from 0 up to 40 Hz. This is done to get a good correlation of wind tunnel propeller speed and the average airflow speed inside the test section of the wind tunnel. The calibrated data is plotted in Figure 7, showing the relationship between speed of wind tunnel propeller blades (Hz) and the speed of airflow (m/s) inside the test section.

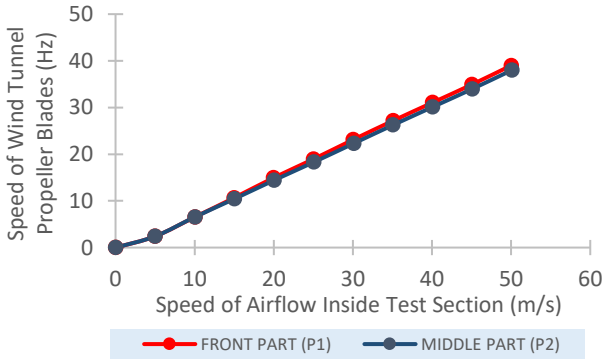

Figure 7 Correlation between the speed of the wind tunnel propeller blades (Hz) and the airflow speed (m/s) inside the test section

There are a few procedures to follow for the wind tunnel test section air flow speed calibration test.

1. To begin, two pitot tubes are placed in the test section, one at the front of the wind tunnel's test section and another at the middle of the test section. The pitot tubes are connected to the digital manometer (Testo 510 Differential Manometer); measure the airflow speed, determined from the differences between the total pressure and the static pressure inside the wind tunnel test section.
2. Then, each pitot tube is connected to a digital manometer, which will show the velocity of airflow, measured in m/s. Other important experimental data are recorded, such as the air density, 1.225 kg/m^3.

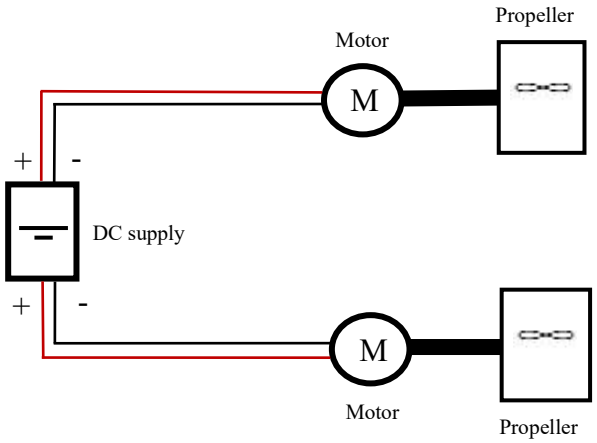

Figure 8 Schematic diagram for the electronic connection.

In this experiment, there are two propellers installed and used to induce the airflow towards the inner-front section of the wing channel, alike the one performs at Georgia Tech Research Institute [23]. The size of the propeller is 4 cm in diameter, it is attached to a small coreless DC motor (rated at 3.7 Volt, 0.1 Amp) that provides thrust force. As shown in Figure 8, there are two small electric motors connected to each of the propeller.

Using a custom-designed mounting stand, the aircraft is installed inside the test section (as shown in Figure 9). During the experiment, the airflow velocity is digitally controlled by a knob on the right-side of the wind tunnel. The measured correlation (done during calibration) between the speed of the wind tunnel propeller blades (Hz) and the speed of the airflow (m/s) inside the wind tunnel test section is used to calculate the airflow speed. All the measured forces are displayed on a computer linked to the wind tunnel's balance system. The data on the monitor shows force and moment measurements for all three axes, with the two forces from the X- and Z-axes representing drag and lift, respectively.

Figure 9 Test model in the wind tunnel test section

III. RESULTS AND DISCUSSION

The aerodynamics lift performance characteristics of a channel-wing model are investigated at various wind speeds (ranging from zero to 22 m/s) and angles of attack (ranging from -10 to +20 degrees, with a 5 degree increment).

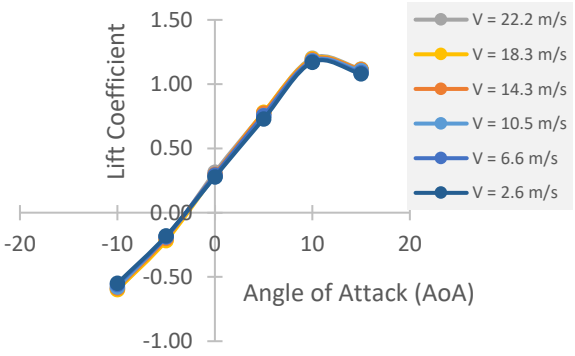

Figure 10 Lift at different AoA (motors OFF)

The results shown in Figure 10 depict the characteristics of the lift produced at various AoA when both electric motors are turned off. The depicted data is similar to the NACA 4412 airfoil lift performance data. The overlapping lines demonstrate that the lift coefficient is independent of free-stream airflow speed. The highest lift coefficient emerges at 10 deg., and everything appears to decrease after that. This is consistent with many established research data; wing with NACA 4412 airfoil profile typically stall above 15 degrees (AoA).

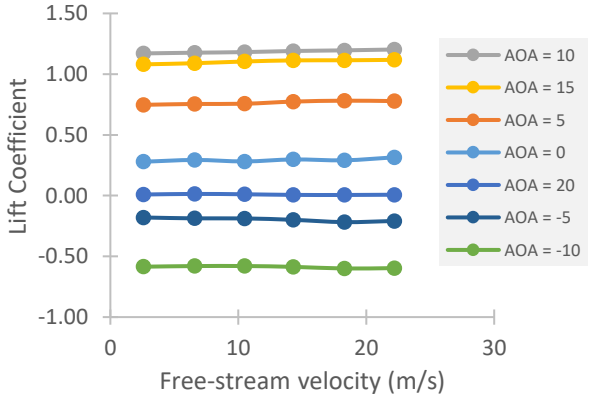

Figure 11 Lift at different free-stream airflow velocity (motors OFF)

Figure 11 depicts the characteristics of the lift produced (when both electric motors are turned off) at various free-stream airflow velocity. The graph shows the value of the lift coefficient remains unchanged and stable across the range of measured free-stream velocity. It demonstrates that the highest lift coefficient emerges at an angle of attack of +10 degrees, while the lowest is observed at -10 degrees; this fits with reported measurement data for a wing with a NACA 4412 airfoil profile.

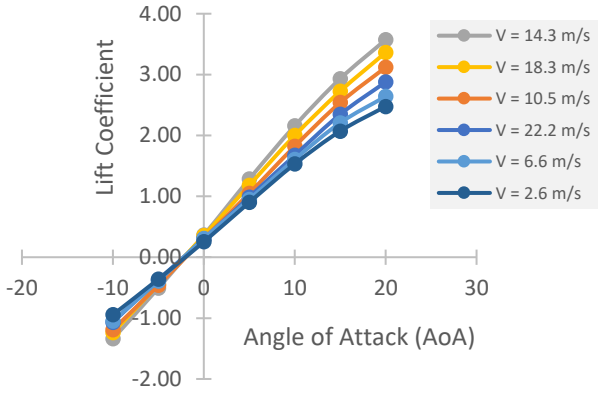

Figure 12 Lift at different AoA (motors ON)

Figure 12 depicts the characteristics of the lift produced at various AoA when both electric motors are activated. The data appears similar to that given in Figure 10, with each line crossing at the same point (on the horizontal axis), at an AoA of around -3 degrees. However, unlike the trend lines for conditions when the electric motors are turned off, the lift coefficient appears to increase further for AoA greater than +10 deg. This is because of the suction force produced by the high-speed rotating propeller blades, air is entrained to the inner section of the wing's channel. The largest lift coefficient can be observed at AoA of +20 degrees, with the lift coefficient reaching 3.5 for a speed of 14.3 meters per second. Following that are 18.3 m/s, 10.5 m/s, 22.2 m/s, 6.6 m/s, and the lowest at 2.6 m/s with a lift coefficient of 2.4.

It is important to note that the low free-stream airflow speed could result in higher lift and appear to delay wing stall. The findings also revealed that the greatest magnitude of airflow does not ensure the greatest lift. This is because increased free-stream airflow velocity reduces flow-turning effects at the trailing edge of the channel-wing. As the magnitude of the free-stream increases, the differences between it and the entrainment caused by the suction from the rotating propeller become less. As a consequence of this, the development of low-pressure region (negative pressure) inside of the channel-wing is reduced; giving an unfavorable affects to the generation of lift. Therefore, a careful consideration to the specific design and sizing of channel-wing is indeed crucial.

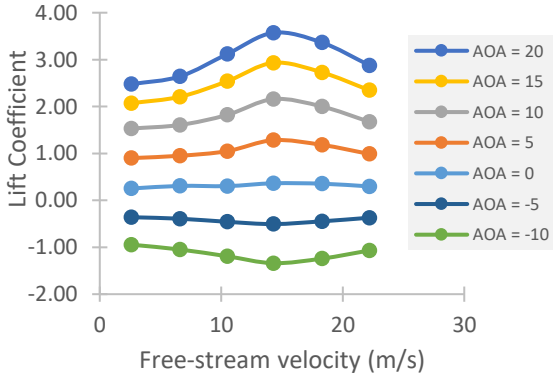

Figure 13 Lift at different free-stream airflow velocity (motors ON)

From the graph in Figure 13 above, it shows the characteristics of the lift produced at different free-stream airflow velocity; when both electric motors are turned on. The air is entrained to the inner part of the wing channel; this is due to the suction effect comes from the high-speed rotating propeller blades. Unlike in Figure 11, the trend lines for each plotted value is different. The magnitude of the lift coefficient produced at any AoA is greater and changing with the free-stream airflow speed. As the electric motor is turned on, the propeller entrained more air to the inside of the channel-wing section. This eventually reduces the pressure along the chord of the channel-wing (promotes low-pressure region on the inside of the channel-wing).

Observing the trends of each line (as shown in Figure 11 and Figure 13), it shows that if the airflow speed is further increased, the lift force produced seems unchanged for condition when the electric motors is turned off. While, for condition when the electric motors are turned on, the lift is reduced for positive AoA, and in the opposite for negative AoA. Noted that, beyond the highest free-stream speed of 22.2 m/s, the tested model experiencing unfavorable conditions, in which the model tends to vibrate excessively; thus, limiting for testing at much higher air speed.

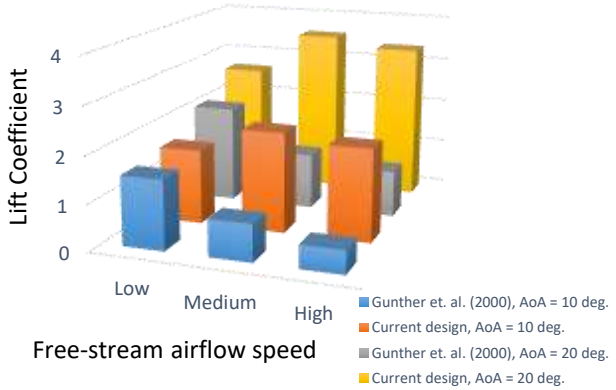

Figure 14 Comparison for cases with different positioning of propulsion unit; inside of the channel-wing (blue, grey), and behind the channel-wing (orange, amber)

Figure 14 compares Gunther et al. [28] data to the current design (for conditions with 10- and 20-deg. AoA). To provide a baseline for comparison, free-stream airflow speeds are defined as low, medium, and high, which correspond to recorded free-stream airflow speeds of about 6 m/s, 13 m/s, and 18 m/s, respectively.

For current design, the model has the propulsion unit positioned behind the channel-wing, whereas Gunther et al. [28] have it on the inside of the wing channel. Due to the positioned on the inside, it produces less lift, and steadily decreasing with speed (Figure 14). This is caused by the region (gap) between the propulsion unit and the channel-wing. It is narrow, causing a blocking effect that worsens with speed, similar to biplane aircraft [29-31]. In this condition, airflow interference is unavoidable; the high-pressure air beneath the propulsion unit interacts with the low-pressure air above the channel-wing surface. Limiting the formation of a low-pressure region inside the channel-wing. In contrast with the present design, the airflow is uninterrupted, the lift is higher, and it rises with speed; the trend is the same in both cases (10- and 20-deg. angles of attack).

IV. CONCLUSIONS

Present study is aiming to acquire the aerodynamic performance for short-haul flights. Analysis is done experimentally with a 3D-printed model. The aircraft wing model is constructed with NACA 4412 profile, wingspan of 400 mm, and U-shape-channel diameter of 68 mm. Tested in an open loop wind tunnel at speed of up to 22 m/s, and angle of attack of up to +20 degrees.

Comparing between electric motors on and off conditions, when it is turned on, lift force can still be produced even beyond the +10 deg.; delaying the separation of airflow and maintaining the lift beyond which the usual state (at higher AoA) where the typical modern wing would stall. The result shows at +20 degrees AoA the lift coefficient can reach beyond 3, higher than those obtained by the conventional wing design.

Furthermore, data suggests that the highest free-stream may not necessarily yield the greatest lift. This is because an increase in free-stream diminishes flow-turning effects at the channel-wing's trailing edge. With increasing free-stream, the local velocity on the inside of the channel-wing is reduced, and the formation of the low-pressure region is gradually shrank. As a result, the generation of lifts is decreased.

The current design also demonstrates that the positioning of the propulsion unit is crucial. Strongly influences the generation of lift (or formation of a low-pressure region on the inside of the wing channel). With the propulsion unit placed behind the channel-wing, the narrow gap obstruction that may impair airflow is no longer a concern. The formation of low-pressure regions on the inside of the wing channel surfaces is enhanced, resulting in higher lift and rises with speed. This could also underline the significance of uninterrupted airflow in ensuring the aircraft's stability. As a result, appropriate guidelines must be set to guarantee that the lift is fully optimized for the design of channel-wing aircraft.

In conclusion, it is vivid that the results gained interprets that the new channel-wing aircraft design is the most suitable candidates for STOL application. It had the ability to produce greater lift than conventional aircraft equipped with modern high-lift systems, and it outperformed the traditional channel-wing design. Furthermore, the channel-wing aircraft has a superior take-off ability at low speed and could perform maneuver at higher AoA.

The amount of data and repeatable runs that could be taken was constrained by tunnel duration and technical challenges. Future study should include a more extensive analysis that considers various parameters as well as new design considerations. Since the model in this study was produced via 3D printing, some modification has to be

made to improve the rigidity of the test model. So that, it can be tested to its absolute limits (which comprises wing stall characteristics). The current work adds to the understanding of the aerodynamic performance of channel-wing aircraft designs, notably the influence of repositioning of the propulsion unit.

ACKNOWLEDGMENTS

The authors would like to thank to the Universiti Putra Malaysia for providing the financial support through the Industry Research Grant, Endowment Tan Sri Syed Azman (6338203-10801).

REFERENCES

[1] Birolini S, Cattaneo M, Paolo M, Chiara M, "Integrated origin-based demand modeling for air transportation," *Transportation Research Part E: Logistics and Transportation Review*, Vol. 142, 2020, DOI: 10.1016/j.tre.2020.102050

[2] Ahmed A, Guzhva VS, "Exploratory Analysis of Air Travel Demand Stimulation in First-Time Served Markets," *Journal of Air Transport Management*, Vol. 98, 2022,
DOI: 10.1016/j.jairtraman.2021.102162

[3] Suh DY, Ryerson MS, "Forecast to grow: aviation demand forecasting in an era of demand uncertainty and optimism Bias," *Transportation Research Part E: Logistics and Transportation Review*, Vol. 128, 2019,
Doi: 10.1016/J.Tre.2019.06.016

[4] Belobaba P, Odoni A, Barnhart C, "The Global Airline Industry," 2009.

[5] Alice S, Jorge S, Diego C, Eduardo O, "On the relevance of data science for flight delay research: A systematic review," *Transport Reviews*, Vol. 41, No. 4, 2021.

[6] O'connell JF, "The global airline industry," In the routledge companion to air transport management, 2018.

[7] Santos BF, Wormer MMEC, Achola TAO, Curran R, "Airline delay management problem with airport capacity constraints and priority decisions," *Journal of Air Transport Management*, Vol. 63, 2017,
Doi: 10.1016/J.Jairtraman.2017.05.003.

[8] Tee YY, Zhong ZW, "Modelling and simulation studies of the runway capacity of Changi Airport," *Aeronautical Journal*, Vol. 122, No. 1253, 2018, Doi: 10.1017/Aer.2018.48.

[9] Thobois L, Cariou JP, Cappellazzo V, Musson C, Treve V, "Comparison and validation of wake vortex characteristics collected at different airports by different scanning Lidar sensors," In Epj Web of Conferences, Vol. 176, 2018,
Doi: 10.1051/Epjconf/201817606002.

[10] Roa J, "Technology Development Framework for Air Traffic Control Assisted Airport Procedures in Dynamic Wake Separations," In Advances in Human Aspects of Transportation: Proceedings of the AHFE 2018 International Conference on Human Factors in Transportation, July 21-25, 2018, Loews Sapphire Falls Resort at Universal Studios, Orlando, Florida, USA 9, 2019, pp. 11-18. Springer International Publishing,
Doi: 10.1007/978-3-319-93885-1_2.

[11] Itoh E, Mitici M, "Evaluating the impact of new aircraft separation minima on available airspace capacity and arrival time delay," *Aeronautical Journal*, Vol. 124, No. 1274, 2020,
Doi: 10.1017/Aer.2019.160.

[12] Hallock JN, Holzäpfel F, "A review of recent wake vortex research for increasing airport capacity," *Progress in Aerospace Sciences*, Vol. 98, 2018,
Doi: 10.1016/J.Paerosci.2018.03.003.

[13] Cappellazzo V, Treve V, Chalon C, Visscher ID, "Design principles for a separation support tool allowing optimized runway delivery," 2018,
Doi: 10.2514/6.2018-4237.

[14] Savoni L, Rudnik R, "Pylon design for a short range transport aircraft with over-the-wing mounted UHBR engines," 2018 AIAA Aerospace Sciences Meeting, Kissimmee, Florida,
Doi: 10.2514/6.2018-0011.

[15] Keane PM, Keane AJ, "Use of Custer channel wings-wing ducts on small UAVs," *Journal of Aerospace Engineering*, Vol. 29, No. 3, 2016, pp. 1-10,
Doi: 10.1061/(Asce)As.1943-5525.0000535.

[16] Nishanth P, Arokkiaswamy A, Alen A, "Shape optimization of blended-wing-body configuration - An experimental approach," *International Journal of Recent Technology and Engineering*, Vol. 8, No. 1, 2019,
Doi: 10.2139/Ssrn.3507300.

[17] Chen Z, et al., "Assessment on critical technologies for conceptual design of blended-wing-body civil aircraft," *Chinese Journal of Aeronautics*, Vol. 32, No. 8, 2019,
Doi: 10.1016/J.Cja.2019.06.006.

[18] Dehpanah P, Nejat A, "The aerodynamic design evaluation of a blended-wing-body configuration," *Aerospace Science And Technology*, Vol. 43, 2015,
Doi: 10.2514/6.2013-2414.

[19] Majeed JN, Mat S, Radzi NHM, "Aerodynamic characteristics and laminar bubble separation study on a generic light aircraft model," *Journal of Aeronautics, Astronautics and Aviation*, Vol. 52, No. 4, 2020,
Doi:10.6125/JoAAA.202012_52(4).01

[20] Chen H, Zhong C, "Airfoil optimization design of tiltrotor aircraft based on the computational fluid dynamics method," *Journal of Aeronautics, Astronautics and Aviation*, Vol. 53, No. 4, 2021,
Doi: 10.6125/JoAAA.202112_53(4).02

[21] Wang H, Gan W, Li D, "An investigation of the aerodynamic performance for a fuel saving double channel wing configuration," *Energies*, Vol. 12, No. 20, 2019,
Doi: 10.3390/En12203911.

[22] Shmilovich A, "Unconventional applications and new approaches for flow control," *Fundamentals of*

High Lift for Future Civil Aircraft, Vol. 145, 2021 DOI: 10.1007/978-3-030-52429-6_1

[23] Englar R, Campbell B, "Pneumatic channel wing powered-lift advanced superstol aircraft," 1st Flow Control Conference, St. Louis, Missouri, 2002, pp. 1-10, Doi: 10.2514/6.2002-3275.

[24] Abbas A, Vicente JD, Valero E, "Aerodynamic technologies to improve aircraft performance," *Aerospace Science and Technology*, Vol. 28, No. 1, 2013, pp. 100-132, Doi: 10.1016/J.Ast.2012.10.008.

[25] Blick EF, Homer V, "Power-on channel wing aerodynamics," *Journal of Aircraft*, Vol. 8, No. 4, 1970, pp. 234-238, Doi: 10.2514/3.44260.

[26] Shafie MAM, Hamid MFA, Rafie ASM, "Circulation control aircraft design: Assessment on the channel-wing lift-thrust performance characteristics," *Journal of Advanced Research in Fluid Mechanics and Thermal Sciences*, Vol. 64, No. 1, 2019, pp. 143-151.

[27] Chang M, Zheng Z, Meng X, Bai J, Wang B, "Aerodynamic analysis of a low-speed tandem-channel wing for eVTOL aircraft considering propeller–wing interaction," *Energies*, Vol. 15, No. 22, 2022.

[28] Gunther C, Marchman J, VanBlarcom R, "Comparison of channel wing theoretical and experimental performance," 38th Aerospace Sciences Meeting and Exhibit, 2000, Doi:10.2514/6.2000-257

[29] Knight M, Carl JW, "Wind-tunnel tests on a series of wing models through a large angle of attack range. Part I: Force Tests," Annual Report-National Advisory Committee for Aeronautics Rept. NACA-TR-317 15, 1929, pp. 255-303.

[30] Gall PD, Hubert CS, "Aerodynamic characteristics of biplanes with winglets," *Journal of Aircraft*, Vol. 24, No. 8, 1987, pp. 518-522.

[31] Traub LW, "Theoretical and experimental investigation of biplane delta wings," *Journal of Aircraft*, Vol. 38, No. 3, 2001, pp. 536-546.

[32] Zilberman M, "Custer Channel Wing (CCW) Phase III," In AIAA Scitech Forum, 2021, pp. 0113.

[33] Bushnell DM, Wygnanski I, "Flow Control Applications," NASA/TM –2020 – 220436, 2020.